proceedings

ISEA 2018
Brisbane Queensland Australia
26-28 March 2018
'Engineering of Sport'

MDPI

Proceedings

A Thermal Test System for Helmet Cooling Studies †

Shaun Fitzgerald *, Henry Atkins, Ryan Leknys and Richard Kelso

School of Mechanical Engineering, the University of Adelaide, Adelaide 5005, Australia; henry.atkins@alumni.adelaide.edu.au (H.A.); ryan.leknys@adelaide.edu.au (R.L.); richard.kelso@adelaide.edu.au (R.K.)

* Correspondence: shaun.fitzgerald@adelaide.edu.au; Tel.: +61-8-8313-3152

† Presented at the 12th Conference of the International Sports Engineering Association, Brisbane, Queensland, Australia, 26–28 March 2018.

Published: 13 February 2018

Abstract: One of the primary causes of discomfort to both irregular and elite cyclists is heat entrapment by a helmet resulting in overheating and excessive sweating of the head. To accurately assess the cooling effectiveness of bicycle helmets, a heated plastic thermal headform has been developed. The construction consists of a 3D-printed headform of low thermal conductivity with an internal layer of high thermal mass that is heated to a constant uniform temperature by an electrical heating element. Testing is conducted in a wind tunnel where the heater power remains constant and the resulting surface temperature distribution is directly measured by 36 K-type thermocouples embedded within the surface of the head in conjunction with a thermal imaging camera. Using this new test system, four bicycle helmets were studied in order to measure their cooling abilities and to identify 'hot spots' where cooling performance is poor.

Keywords: thermal comfort; bicycle helmets; human mannequin; cycling

---

1. Introduction

A major cause of discomfort to both professional and recreational cyclists is overheating of the head during high exertion cycling, with one study citing that 20% of adults who do not use a helmet do so due to discomfort created by excessive over heating [1]. All cycling helmets, some to a greater extent than others, have methods of providing cooling to the head through the use of venting holes and channels. These typically draw airflow across the scalp, transporting heat away from the head through forced convection. However, there is no standard design that provides optimum cooling; rather a myriad of helmet designs are available. Additionally, each helmet has to balance the often contradictory goals of safety, effective cooling and low aerodynamic drag, leading to further variations in shape. One method of determining the cooling effectiveness of a particular helmet is with a thorough investigation of its thermal response in a controlled environment.

The efficacy of a helmet's cooling ability is generally measured quantitatively through the use of a heated mannequin headform in a wind tunnel which provides convective cooling. A headform constructed by Brühwiler [2] from a polyester fashion mannequin is split into three independently heated areas, two of which are monitored for investigations. Each area is maintained at a constant temperature measured by resistance wires on the head surface. The subsequent input power required to maintain constant temperature conditions corresponds to the heat losses of the head. This headform produces sweat through pores at a computer-controlled and regulated flow rate. An additional headform, which functions in an analogous manner to the Brühwiler head, has also been developed and tested by Martínez et al. [3], however this newer headform is constructed from a carbon-fibre/epoxy matrix and is split into nine thermal zones. This allows greater quantification of the local heating efficiency of helmets with a clear distinction in the cooling power differentials between alternate zones. A headform developed by Alam et al. [4] attaches a heater pad and nine thermocouples externally to a fashion mannequin head. The heater mat is heated to 56 °C in still air and the temperature drop is monitored for five minutes when the head is placed in a wind tunnel. A different method is demonstrated by Reid and Wang [5] who used a headform constructed from aluminium filled cast urethane that was heated at a constant power. The cooling effectiveness was directly compared to that of a bare sphere measured simultaneously. The temperature on the headform was recorded with 13 thermocouples and a weighting scheme was used to determine the average temperature of the whole head. A number of commercial helmet manufacturers have also designed their own heated heads but limited information on these is available. Generally they are similar to the previously described headforms, constructed from aluminium, and incorporate varying numbers of thermocouples.

The headform presented in the current article utilizes aspects of the apparatuses discussed above to produce a new headform to measure the cooling efficiency of cycling helmets. The authors present an alternative headform design that can detect and measure detailed thermal gradients of the scalp. This headform is constructed from 3D printed ABS plastic that is heated at a constant power whilst the temperature drop, when placed in a wind tunnel, is monitored using 36 thermocouples embedded in the headform surface.

2. Mannequin Head Design & Usage

2.1. Materials of Constuction

As a cyclist's head is cooled via airflow channeled through vents in their helmet, there can be large variations in the local head temperature depending on the location of these vents. A study by De Bruyne et al. [6] observed spatial differences of up to 5.5 °C between different areas of the head. Hence a focus in the design of this headform was for the ability to adequately replicate and observe the various hot and cold regions that a human head would experience during cycling. These temperature gradients are attenuated via lateral conduction across the scalp. The rate of this heat transfer is the conduction heat flux q'' (Wm^{-2}) and is given in Equation 1 where k ($Wm^{-1}\,K^{-1}$) is the thermal conductivity of the material and ΔT (K) is the change in temperature. The value for k for various materials used previously to construct heated headforms are presented in Table 1 alongside estimated k for human flesh. As a head has a relatively low thermal conductivity it does not distribute heat evenly over the scalp, rather the local temperature can vary considerably from the average temperature. In order to adequately resolve the temperature distribution across the scalp, a thermal conductivity close to that of a human head was a primary factor in material choice. Acrylonitrile Butadiene Styrene (ABS) has a value for k close to but slightly lower than any natural human material and hence would encourage the creation of local hot spots. This facilitates the design and evaluation of cycling helmets, as the effectiveness of cooling vents can clearly be seen in thermal images or temperature maps. Using a material with a high thermal conductivity, such as aluminium or copper, would result in high heat dissipation with any localized hot spots quickly dissipating over the entire head, obscuring finer cooling details.

$$q'' = -k\Delta T, \quad (1)$$

Table 1. The thermal conductivity of generic headform materials and human body parts at 300 K [7,8].

Material	Thermal Conductivity—k ($Wm^{-1}\,K^{-1}$)
ABS Plastic	0.17
Aluminium Alloy/Pure	168–237
Copper—Pure	401
Carbon Fiber/Epoxy—parallel to fibers	11.1
Carbon Fiber/Epoxy—perpendicular to fibers	0.87
Human skin	0.29–0.54
Human muscle	0.2–0.5
Human bone	0.41–0.63

2.2. Head Geometry

The external geometry of the headform was obtained from a survey by Zhuang and Bradtmiller [9] that measured head and facial dimensions of 3997 subjects in conjunction to scanning 1013 of the subjects with a 3D scanner. Averaged 3D models of five different heads of standard sizes were created from this data, with the 50th percentile head size being obtained by the authors. This head model was scaled by a minor factor such that it fitted a typical 58 cm medium cycling helmet and this provided the surface for instrument installation. The head was split along the reference plane of a K-type headform [10], and as such defines the head region typically covered by a cycling helmet. The top half had 36 evenly and symmetrically spaced holes across the surface of the scalp for the placement of thermocouples. The lower half had solid mounting points located near the lower ear lobe and on the inside surfaces of the neck region. This enabled mounting of the headform to a fixed stand at multiple inclination angles. Each half was 3D printed in 4 mm thick ABS plastic.

2.3. Headform Design

A cross-sectional diagram depicting the headform construction is given in Figure 1 and a detailing of the design is to follow. A heater mat is cut and moulded so that it sits flush with the inner-surface of a mix of epoxy resin and aluminium particles with a uniform thickness of 10 mm. This resin is rich in aluminium and completely fills the area between the surfaces of the heater mat and ABS scalp, providing a high thermal mass to ensure an even heat transfer from the heater mat to the scalp. An aluminium plate underneath the heater conducts heat to the base of the ABS scalp, preventing heat loss down to the un-heated lower head. A thermal insulating layer helps to further contain the heat within the scalp. The void inside the scalp is filled with a polyester packing material to ensure that the aluminium-epoxy mix and heater-mat are firmly pressed against the inside surface of the ABS, thus maximizing the heat transfer to the surface. A K-type thermocouple is placed flush with the surface in each hole in the mannequin, with the wires directed through the internals of the headform and out of the bottom of the neck.

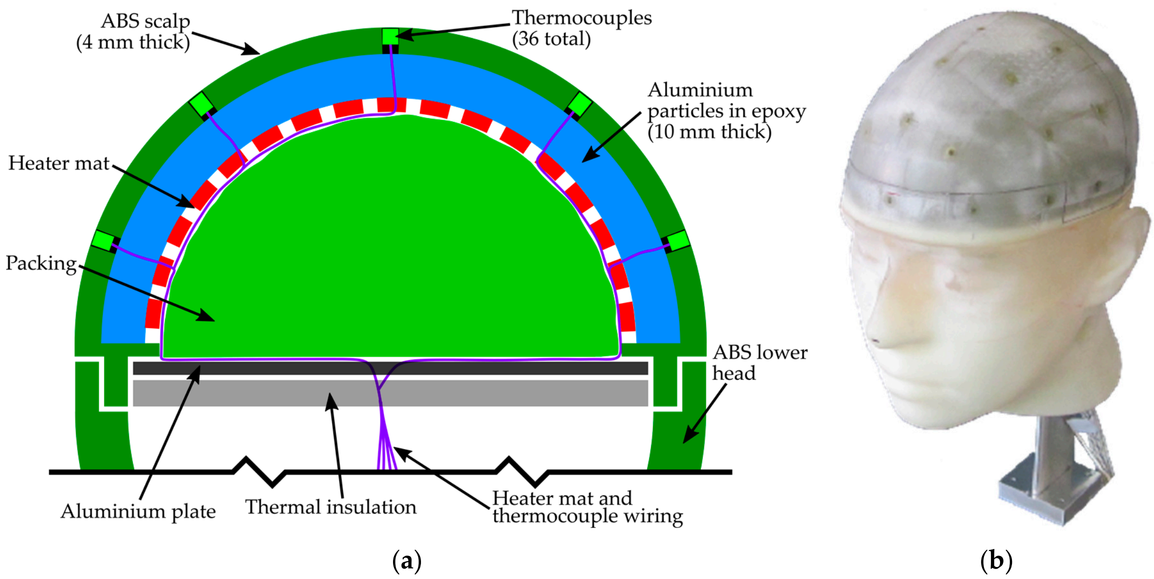

Figure 1. (**a**) Cross-sectional view of the heated headform detailing the construction. (**b**) Final fabricated headform, prior to being painted black.

2.4. Errors

The greatest source of error in this headform originates in the thermocouple measurements. The K-Type thermocouples are standard limits of error with an accuracy of ±2.2 °C. However, this error is minimized when calculating the average temperature of the entire head due to the large quantity and wide area of all 36 thermocouples. Additionally, the thermal camera can be used as a second source of temperature data to corroborate the temperature recorded by the thermocouples. It was found the thermal camera consistently calculated approximately a 2 °C lower maximum temperature values than the thermocouples. This is likely due to the short time delay between taking the helmet off and capturing the two thermal images. Thermal testing was repeated for several helmets and the results were repeatable to within ±0.62 °C. Testing was not conducted within an environmental chamber, however the temperature was monitored throughout all testing, where it remained constant at 24.9 °C with a standard deviation (SD) of 0.50 °C.

3. Results and Discussion

3.1. Description of Helmets

Testing of the thermal head was conducted on the bare head (BH) as well as four bicycle helmets. These are a Time Trial helmet (TT), an older-generation road cycling helmet (VR), and two modern aero-road helmets designed for both speed and thermal cooling (AR1 & AR2). For purposes of anonymity the exact details and branding of the helmets have been obscured.

3.2. Thermal Testing

Testing of the thermal properties of the helmets was completed in The University of Adelaide's KC Wind Tunnel. This is a low speed open-jet wind tunnel with a 0.5 × 0.5 m test section and maximum speed of 30 m/s. The thermal head mannequin was heated until it achieved a constant average temperature of 38 °C in still air. The heater mat power supply was then constantly maintained at this power output throughout testing. Experimentation was completed with the head angled 30° from the vertical plane and at a velocity of 11 m/s. For each helmet the temperature data from the thermocouples was constantly recorded, with steady state conditions being achieved after 40 min. After 50 min the wind tunnel was turned off and the test section outlet was blocked to prevent further airflow on the mannequin head. The helmet was then removed, and a thermal image of the headform taken from the front and the rear. This final process was performed over a short period of time, as once the tunnel was turned off and the helmet removed, the heat would begin to dissipate in a manner not representative of typical cycling conditions. However, due to the low thermal conductivity of the ABS headform, there was adequate time to capture the thermal images without loss of fine heat spot details.

A top view of the headform was created by projecting the 3D location of each of the thermocouples onto a 2D plane. Delaunay triangulation was then used to interpolate the thermocouple temperature values at these points and produce a distribution map of the head surface temperature. This provides a clear and consistent method of finding the temperature at any point across the head surface. It is also used to correlate the temperature distribution patterns seen in thermal images of the headform. However, this representation has limitations due to the impossibility of replicating a 3D surface on a 2D plane.

Thermal images of the mannequin from the front and rear are displayed in Figure 3. Of note in these images, as well as the contour plots, are variations of the temperature across the scalp surface where cooling has been effective to different levels. Across all test conditions, there was an average temperature difference of 9.2 °C between thermocouples with a maximum temperature difference of 25 °C between two points of the head in the TT helmet, as shown in Figure 2. This is a much larger discrepancy than found by De Byrne et al. [6]. One cause of the variation in temperature is due to the frontal thermocouples generally being located below the helmet brim and directly in the airflow, producing much lower temperature values compared to points completely insulated from both the free-stream and alternative cooling flows provided by the helmets. However, this is beneficial for a helmet comparative tool as it provides a clear indication of areas where cooling is effective.

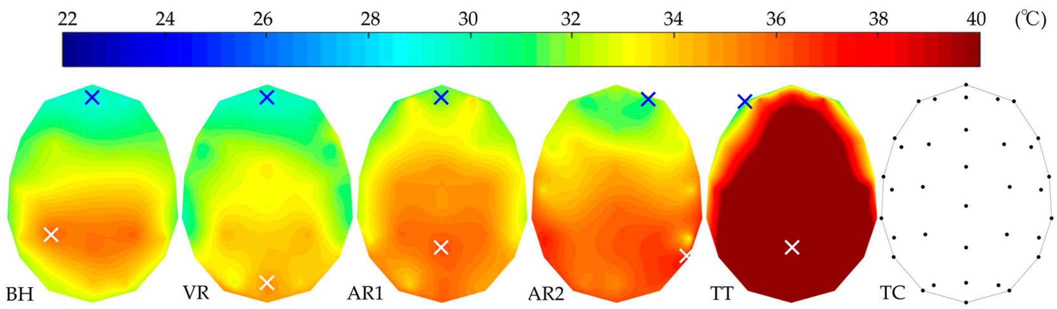

Figure 2. Contour plots of the temperature across the mannequin headform for four different style cycling helmets and the bare headform. The blue and white crosses are the locations of the minimum and maximum temperature respectively. Diagram TC displays the location of each thermocouple.

The TT helmet was the only helmet that increased in head temperature over the course of the 50 min test. The cooling of this helmet is so ineffective that even with a 40 km/h breeze, the helmet insulated the scalp from any convective cooling, resulting in the head temperatures to increase higher than if it was open and exposed to still air. In contrast, helmet VR provided very efficient heat transfer mechanisms, cooling the headform to lower than BH. Observations of the thermal images for helmets AR1 and AR2 shows distinctive variations in head temperature with much greater cooling properties being located towards the front, rather than the rear of the headform. Also visible in Figure 3 are lines of warm and cool spots which replicate the helmets underside alternating between padding and airflow channels.

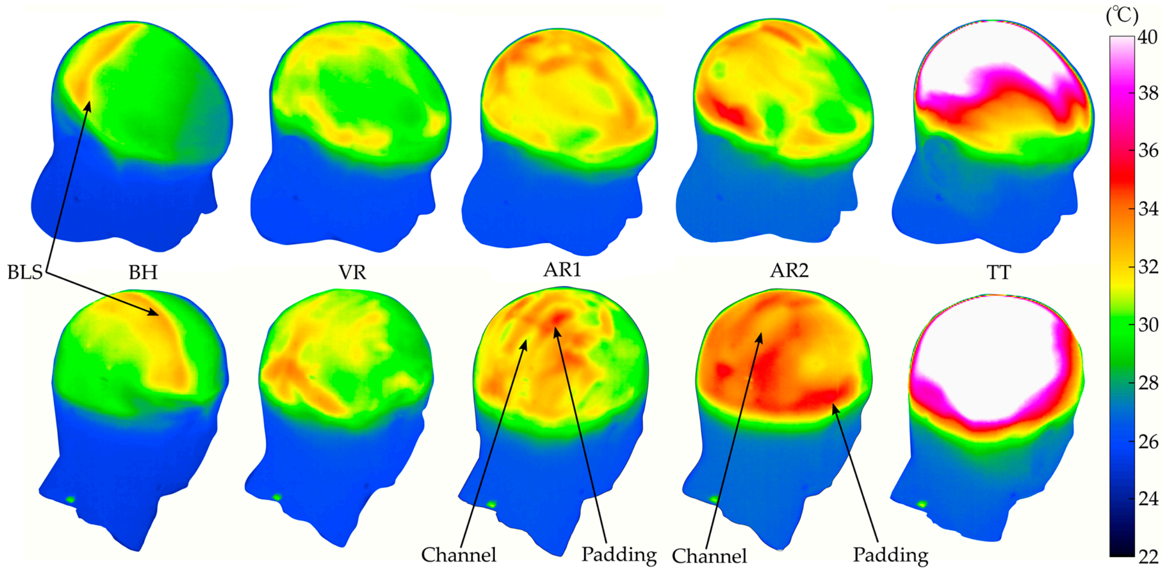

Figure 3. Front and rear thermal images of the heated head at the end of testing, shortly after the helmet has been removed. The clear line on BH is the point of boundary layer separation.

4. Limitations

This heated headform performs well in measuring the thermal properties of cycling helmets, however there are avenues for improvement. The effects of sweating on the convective heat transfer is not able to be investigated in this design. Additionally, the influence of hair would potentially have a large impact on the thermal cooling abilities of helmets, particularly if the hair did not lie flat on the scalp but rather projected into the vents and channels inside the helmet. For the headform to be used for other purposes, such as for the cooling of cricket or motorcycle helmets, the lower face and head would require heating and instrumentation to resolve the temperature gradients in the respective regions. This is not an issue in cycling as the only area covered by a helmet is the top of the head which is monitored by this headform. The headform in the current study has not been validated with human studies and as of yet cannot be used as a direct representation of the heat experienced by a live cyclist. However, it performs well as a helmet cooling comparison tool for design and evaluation of general purpose and advanced cycling helmet designs.

5. Conclusions

A heated headform for investigating the cooling effectiveness of cycling helmets has been constructed and tested on four elite helmets. This headform is constructed from an ABS that exhibits a similar thermal conductivity to human skin, therefore allowing local hot and cold spots to be observed. Testing is completed by heating the headform at a constant power and mapping the temperature across the scalp with 36 thermocouples embedded within its outer surface. This headform provides a clear visual and analytical indication of the local cooling effectiveness of different sized and located vents through recording the localized heat distributions.

Acknowledgments: This research was supported by Scott Sports SA. The authors would also like to acknowledge the help of Paul Grimshaw, Darcy Thompson-Bagshaw, Tom Goddard, Guy Page and Ben Whyte.

Conflicts of Interest: The authors declare no conflict of interest and the funding sponsors had no role in the design of the study; in the collection, analyses, or interpretation of data; in the writing of the manuscript and in the decision to publish the results.

References

1. Finnoff, J.T.; Laskowski, E.R.; Altman, K.L., Diehl, N.N. Barriers to bicycle helmet use. *Pediatrics* **2001**, *108*, e4, doi:10.1542/peds.108.1.e4.
2. Brühwiler, P. Heated, perspiring manikin headform for the measurement of headgear ventilation characteristics. *Meas. Sci. Technol.* **2003**, *14*, 217–227, doi:10.1088/0957-0233/14/2/309.
3. Martinez, N.; Psikuta, A; Rossi, RM.; Corberan, JM.; Annaheim, S. Global and local heat transfer analysis for bicycle helmets using thermal head manikins. *Int. J. Ind. Ergon.* **2016**, *53*, 157–166, doi:10.1016/j.ergon.2015.11.012.
4. Alam, F.; Chowdhury, H.; Elmir, Z.; Sayogo, A.; Love, J; Subic, A. An experimental study of thermal comfort and aerodynamic efficiency of recreational and racing bicycle helmets. In Proceedings of the 8th Conference of the International Sports Engineering Association, Vienna, Austria, 12–16 July 2010; pp. 2413–2418.
5. Reid, J.; Wang, E.L. A system for quantifying the cooling effectiveness of bicycle helmets. *J. Biomech. Eng.* **2000**, *122*, 421–431, doi:10.1115/1.1287163.
6. De Bruyne, G.; Aerts J.; Van der Perre, G.; Goffin, J.; Verpoest, I.; Berckmans, D. Spatial differences in sensible and latent heat losses under a bicycle helmet. *Eur. J. Appl. Physiol.* **2008**, *104*, 719–726, doi:10.1007/s00421-008-0828-1.
7. Incropera, F. Dewitt, D. Bergman, T. Lavine, A. *Principles of Heat and Mass Transfer*, 7th ed.; John Wiley & Sons: Hoboken, NJ, USA, 2014.
8. Cohen, M. Measurement of the thermal properties of human skin. A review. *J. Investig. Dermatol.* **1977**, *69*, 333–338.
9. Zhuang, Z.; Bradtmiller, B. Head-and-Face Anthropometric Survey of U.S. Respirator Users. *J. Occup. Environ. Hyg*. **2005**, *2*, 567–576, doi:10.1080/15459620500324727.
10. Standards Australia. *Methods of Testing Protective Helmets*; AS/NZS 2512; Standards Australia: Sydney, Australia, 2009.